Caveolin-1 expression and cavin stability regulate caveolae dynamics in adipocyte lipid store fluctuation

Nolwenn Briand, Cecilia Prado, Guillaume Mabilleau, Françoise Lasnier, Xavier Le Liepvre, Jeffrey Covington, Eric Ravussin, Soazig Le Lay, Isabelle Dugail

Nolwenn Briand,[1] Cécilia Prado,[1] Guillaume Mabilleau,[2] Françoise Lasnier,[1] Xavier Le Lièpvre,[1] Jeffrey D. Covington,[3] Eric Ravussin,[3] Soazig Le Lay,[4] and Isabelle Dugail[5]

Caveolin-1 Expression and Cavin Stability Regulate Caveolae Dynamics in Adipocyte Lipid Store Fluctuation

Diabetes 2014;63:4032–4044 | DOI: 10.2337/db13-1961

Adipocytes specialized in the storage of energy as fat are among the most caveolae-enriched cell types. Loss of caveolae produces lipodystrophic diabetes in humans, which cannot be reversed by endothelial rescue of caveolin expression in mice, indicating major importance of adipocyte caveolae. However, how caveolae participate in fat cell functions is poorly understood. We investigated dynamic conditions of lipid store fluctuations and demonstrate reciprocal regulation of caveolae density and fat cell lipid droplet storage. We identified caveolin-1 expression as a crucial step in adipose cell lines and in mice to raise the density of caveolae, to increase adipocyte ability to accommodate larger lipid droplets, and to promote cell expansion by increased glucose utilization. In human subjects enrolled in a trial of 8 weeks of overfeeding to promote fattening, adipocyte expansion response correlated with initial caveolin-1 expression. Conversely, lipid mobilization in cultured adipocytes to induce lipid droplet shrinkage led to biphasic response of cavin-1 with ultimate loss of expression of cavin-1 and -3 and EHD2 by protein degradation, coincident with caveolae disassembly. We have identified the key steps in cavin/caveolin interplay regulating adipocyte caveolae dynamics. Our data establish that caveolae participate in a unique cell response connected to lipid store fluctuation, suggesting lipid-induced mechanotension in adipocytes.

Caveolae are small flask-shaped invaginations of the plasma membrane (1) that are found with remarkable abundance in endothelial cells, myotubes, and adipocytes. They are considered a subset of the so-called lipid raft domains and segregate a number of membrane-related processes (2). An accepted paradigm is that caveolae formation is primarily driven by the assembly of a cytoplasmic coat consisting of oligomeric caveolins (3), a protein family with 3 highly-related members (caveolin-1 through -3). Invalidation of individual caveolin genes led to the generation of mice models lacking caveolae in all cell types or in a tissue-restricted manner (4). Caveolin-1–null mice, which also lack caveolin-2, suffer from severe vascular dysfunction and pulmonary defects (5,6) and develop lipodystrophy (7), a metabolic phenotype that cannot be reversed by endothelial caveolin reexpression, pointing to an important function of adipocyte caveolae (8). Closely related lipodystrophic diabetes is also present in patients with nonsense mutations for caveolin-1 (9).

Despite early evidence for defective mechanotransduction in blood vessels of caveolin-deficient mice (10), the physiological function of caveolae remained debated until recent discovery of a unifying caveolar function as mechanosensors, revealed by their property to respond to membrane tension by flattening into the plasma membrane (11). Another recent breakthrough came from the identification of novel caveolae adaptors named cavins, such as polymerase I and transcript release factor (PTRF)/cavin-1 required

[1]INSERM, U872, Equipe 8, Paris, France
[2]Service Commun d'Imageries et d'Analyses Microscopiques, Université d'Angers, Angers, France
[3]Pennington Biomedical Research Center, Baton Rouge, LA
[4]INSERM, UMR1063, Université d'Angers, Angers, France
[5]INSERM, U1166, Equipe 6, Paris, France

Corresponding author: Isabelle Dugail, isabelle.dugail@crc.jussieu.fr.

Received 31 December 2013 and accepted 20 June 2014.

This article contains Supplementary Data online at http://diabetes.diabetesjournals.org/lookup/suppl/doi:10.2337/db13-1961/-/DC1.

S.L.L. and I.D. equally contributed as co–senior authors.

for caveolae formation (12,13). Specifically enriched in caveolae preparations from human adipocytes (14), PTRF/cavin-1 gene invalidation in mice led to absence of caveolae and lipodystrophic phenotype comparable with the one observed for caveolin-1 knockout mice (7,15). Similarly, PTRF/cavin-1 mutations were identified in human patients suffering lipodystrophic syndromes coupled with muscular dystrophy (16–18), states for which caveolin mutations have also been reported (9,19). Three other cavin homologs were identified (14) and have all been linked to caveolae dynamics (20–23). Despite major importance in regulating caveolae (24), their precise role in mechanosensing still remains unknown.

As caveolae are being recognized as specialized structures responding to plasma membrane tension, it makes sense that a high density of caveolae is found in cells that are physiologically submitted to mechanical stress. These include vascular endothelium in which shear stress is applied by blood circulation, as well as skeletal muscle through contraction-induced stretching. Despite remarkable enrichment in caveolae, estimated to cover ~30–50% of their cell surface (25), adipocytes are not generally considered particularly exposed to external mechanical forces, as they mostly participate in lipid metabolism and energy storage. Indeed, adipocyte morphology is dominated by a central unilocular lipid droplet that fills almost the entire fat cell volume, leaving other organelles including the nucleus at cell periphery. Close apposition of adipocyte lipid droplet to plasma membrane is obvious by electron microscopy, with cytoplasmic thickness as low as 300 nm. Another consequence of the storage compartment being the most prominent intracellular organelle with unusually large dimensions (up to 100 μm diameter in obese patients), the lipid droplet size also resolves overall fat cell volume. As a mirror of highly variable energy status, the adipocyte lipid droplet can be subjected to drastic fluctuations, as well as fat cell size. For example, adipose cell diameter, an easily accessible parameter on adipose tissue histological sections, can vary over a twofold range, which translates into an eightfold change in cell volume. In this context, we reasoned that the lipid droplet organelle might be a driving force for mechanical constrains exerted on the adipocyte plasma membrane, to which caveolae might respond. To examine this possibility, we have designed in vitro cell conditions and in vivo experimental settings in mice and humans, in which caveolae dynamics and/or lipid stores could be manipulated. Our data establish a mutual link between caveolae density and adipocyte lipid stores and reveal that lipid droplet to membrane signaling mechanisms can sense lipid store variations via caveolae. These results therefore suggest that lipid droplets might be viewed as mechano-active organelles in adipocytes.

RESEARCH DESIGN AND METHODS

Materials

Antibodies against caveolin-1, PTRF, and β-actin were from BD Biosciences; EHD2 from Abcam; SDPR/cavin-2 from R&D Systems. Horseradish peroxidase anti-rabbit, -mouse, and -goat IgGs were from Jackson ImmunoResearch Laboratories.

Cell Culture

3T3-L1 cells (J. Pairault, CNRS, Paris, France) maintained in high-glucose DMEM with 10% FCS were induced to differentiate by adding isobutylmethylxanthine (100 μmol/L), dexamethasone (0.25 μmol/L), and insulin (1 μg/μL) for 2 days and then cultured with insulin alone. Differentiated adipocytes were transduced with an adenovirus encoding canine Cav1. Growing 3T3-L1 cells were transduced with retroviral supernatants from Phoenix packaging cells (Indiana University National Gene Vector Biorepository, Indianapolis, IN) expressing Cav1-RFP, PTRF-eGFP, or SRBC-eGFP in pBabe vectors, followed by selection for puromycin resistance (6 μg/mL). Populations of antibiotic-resistant 3T3-L1 fibroblasts were allowed to differentiate into adipocytes as described above.

De Novo Fat Pad Formation in Nude Mice and Immunohistochemistry

Animal studies were approved by the Ethics Committee in Animal Experiment Charles Darwin (agreement no. Ce5/2011/015). 3T3-F442A preadipocytes were grown to near confluence and trypsinized, and cells in PBS were injected subcutaneously (3×10^7 cells per site) in 6-week-old BALB/C NU/NU athymic mice (Charles River Laboratories). Four weeks after implantation, mice on a standard diet received drinking water containing 30% sucrose. At 14 weeks, mice were killed by cervical dislocation and fat pads were excised. Small pieces of adipose tissues were either fixed with paraformaldehyde 4% or homogenized in lysis buffer for Western blotting. Adipose tissues were processed for immunohistochemistry as previously described (8). Adipocyte diameters were measured using ImageJ software.

Overfeeding Study

Thirty-five participants (29 male, 6 female; 20 Caucasian, 14 African American, and 1 other race; with mean ± SD for age 26.7 ± 5.3 years and BMI 25.5 ± 2.2 kg/m^2) were recruited into the overfeeding study. All were provided written informed consent, all study parameters were approved by the institutional review board, and procedures were followed with regard to the Declaration of Helsinki and registered as a clinical trial. Participants consumed a diet of 44% fat, 15% protein, and 41% carbohydrate, where the total daily intake equated to 140% of their normal caloric intake for 8 weeks. Body composition was assessed by DEXA (QDR 4500A; Hologics, Bedford, MA). Under fasting conditions, subcutaneous adipose tissue was collected by Bergstrom needle biopsy for the measurement of fat cell size according to the methodology of Hirsch and Gallian (26) and determination of caveolin-1 protein content.

Glucose Uptake

2-Deoxyglucose uptake was measured in differentiated 3T3-L1 adipocytes as previously described (27).

Lipolysis

Differentiated adipocytes were treated as previously described (28), and glycerol release into the medium was measured using a commercial kit (glycerol, GY105; Randox Laboratories).

Detergent-Resistant Membrane Preparation

3T3-L1 differentiated cells were washed three times with ice-cold PBS and homogenized into 25 mmol/L Mes (pH 6.0), 150 mmol/L NaCl, and 1% (w/v) Triton X-100 containing complete protease inhibitor cocktail (Roche). Detergent-resistant membrane preparations were isolated as previously described (29).

Western Blotting

Samples were lysed (in 50 mmol/L Tris, pH 7.4; 0.27 mol/L sucrose; 1 mmol/L Na-orthovanadate, pH 10; 1 mmol/L EDTA; 1 mmol/L EGTA; 10 mmol/L Na-β-glycerophosphate; 50 mmol/L NaF; 5 mmol/L Na-pyrophosphate; 1% [w/v] Triton X-100; 0.1% [v/v] 2β-mercaptoethanol; and protease inhibitors), centrifuged (15,000*g*, 4°C, 10 min), and stored at −20°C. Protein concentrations were determined by a Bio-Rad kit, and samples were subjected to SDS-PAGE and blotted according to standard procedures. Protein signals were visualized using enhanced chemiluminescence (Perbio Science; Thermo Scientific).

Fluorescence Imaging

3T3-L1 on coverslips were fixed as previously described (30), stained with 0.1 μg/mL LD540 (C. Thiele, University of Bonn, Bonn, Germany), and visualized by confocal laser fluorescence (Zeiss LSM 710). Fluorescence quantification was performed using ImageJ software.

Electron Microscopy

3T3-L1 adipocytes were fixed by 2.5% glutaraldehyde in 0.1 mol/L cacodylate (pH 7.4) and processed as previously described (31). Ultra-thin sections were observed with a JEOL JEM-1400 microscope equipped with a digital camera.

Statistical Analysis

Statistical analysis used Student *t* test, variance analysis, or Spearman regressions for correlations. Data were considered statistically significant at P values <0.05.

RESULTS

Caveolin-1 Overexpression Increases Caveolae Density and Promotes Adipocyte Insulin Response

Indirect evidence for a link between adipocyte lipid droplet expansion and caveolae dynamics is provided by defective lipid storage phenotype of caveolin/caveolae-deficient adipocytes in mice or humans. To examine whether a reciprocal relationship could be demonstrated in gain-of-function experiments, we overexpressed caveolin-1 in fat cells. Because adipocytes already express substantial levels of caveolins, we used a strong cytomegalovirus promoter to drive stable expression of a Caveolin-RFP (Cav1-RFP) fusion in 3T3-L1 adipocytes from retroviral vectors (Fig. 1*A*). Exogenous Cav1-RFP, as well as endogenous cav1, mainly distributed in detergent-resistant membranes after triton ×100 extraction indicating targeting in lipid rafts domains (Fig. 1*B*). By probing with caveolin-1 antibody, we estimated that exogenous Cav1-RFP represented approximately half of the endogenous cav1 cell content, indicating significant (1.5–2.0-fold) but moderate overexpression (Fig. 1*B*). Cav1-RFP distributed to the cell surface of terminally differentiated 3T3-L1 adipocytes consistent with caveolae distribution, even if some punctuate labeling evoking intracellular vesicles could also be observed (Fig. 1*C*), consistent with lipid raft formation and recycling in Golgi membranes (32). Forced expression of Cav1-RFP had no impact on endogenous expression of caveolin-2 or cavin mRNA (Fig. 1*D*) but increased PTRF/cavin-1 protein by 1.5-fold (Fig. 1*E* and Supplementary Fig. 1*A*). Adipose differentiation program was not affected as judged by unaltered levels of key adipogenic transcription factors, lipogenic mRNAs (Fig. 1*F*), and protein expression in a differentiation time course (Supplementary Fig. 1*B*). We next examined whether forced caveolin-1 expression could increase caveolae density at the cell surface, evaluated as the number of caveolae invaginations found in a linear plasma membrane stretch on electron microscopy images (Fig. 1*G*). We observed comparable caveolae density in 3T3-L1 cells and tissue sections of mice adipose tissue, validating relevance of the 3T3-L1 model. Compared with control cell lines (stably transduced with an empty retroviral vector), caveolae density was increased significantly in Cav1-RFP cell lines and approached values found in endothelial cells evenly identified in adipose tissue sections (Fig. 1*H*). We also observed slight enrichment of PTRF/cavin-1 in detergent-resistant membrane fractions of Cav1-RFP cell lines (Supplementary Fig. 1*C*). These data are consistent with previous studies in mice (15) indicating that caveolae structures depend on cavin-to-caveolin ratios. Thus, in the absence of overt effects on fat cell differentiation, moderate caveolin overexpression in 3T3-L1 produced surface caveolae-enriched adipocytes, providing a suitable system to investigate relationships with lipid droplet dynamics. Because caveolin-deficient adipocytes are severely insulin resistant (7), caveolae are viewed as positive regulators in insulin signaling. We therefore examined whether ameliorated insulin response associated with elevated caveolae density in Cav1-RFP adipocytes. Contrary to chronic caveolin-1 deficiency in which loss of adipocyte insulin receptors has been reported (31), we detected no change in insulin receptor, insulin receptor substrate (IRS)-1, or extracellular signal–related kinase (Erk)-1/2 expression, but slightly increased protein kinase B (PKB) mRNA and protein contents were present in Cav1-RFP adipocytes (Fig. 2*A* and *B*). In dose-response experiments, Cav1-RFP cell lines exhibited increased basal phosphorylation of IRS-1, PKB, and Erk-1/2 (Fig. 2*C–E* and Supplementary Fig. 2*A*), which translated into elevated phosphorylation upon insulin stimulation. Basal and insulin-stimulated glucose transport was also higher in Cav1-RFP compared with control adipocytes (Fig. 2*F*). Subsequent glycolytic-dependent lactate production

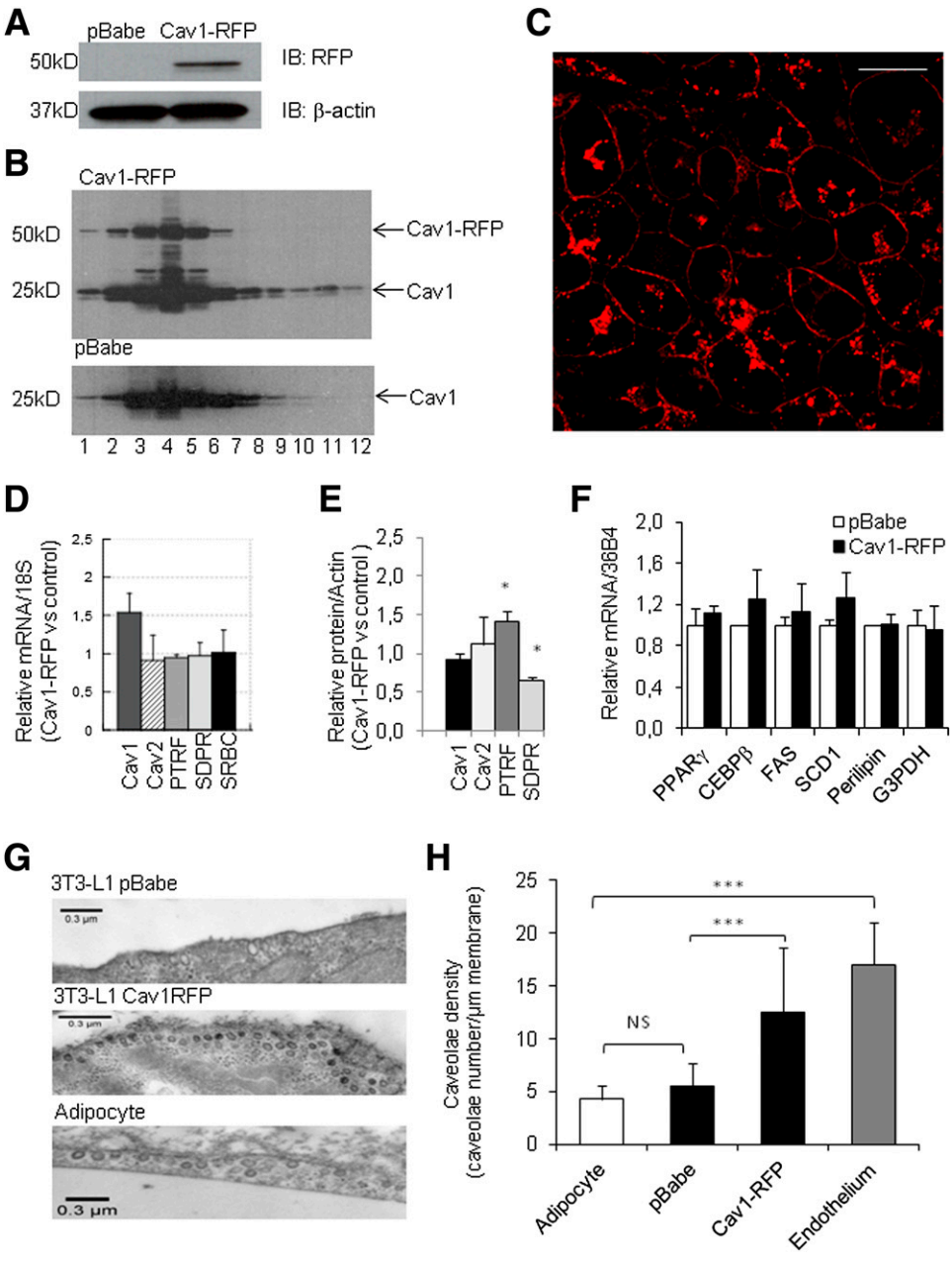

Figure 1—Caveolin-1 overexpression in 3T3-L1 increases adipocyte caveolae density. *A*: Cav1-RFP transgene expression in cells transduced with retroviral constructs containing empty vector (pBabe) or a caveolin-1 cDNA fused to RFP. Membranes were immunoblotted (IB) with an anti-RFP antibody or β-actin. *B*: Endogenous caveolin-1 and exogenous Cav1-RFP distribution into detergent-resistant membrane fractions. Cells stably expressing an empty pBabe vector or Cav1-RFP were lysed in the presence of cold Triton X-100. Detergent-resistant (fraction 1–5) or detergent-soluble (fraction 7–12) fractions were obtained after gradient centrifugation. *C*: Fluorescent imaging of Cav1-RFP cell lines by confocal microscopy. Bar scale is 20 μm. *D* and *F*: Relative mRNA expression in Cav1-RFP versus control cell lines. Indicated mRNA levels were measured by RT-QPCR and normalized to 18S or 36B4 mRNA. Values are means ± SEM obtained in three independent pools of antibiotic-selected clones. *E*: Relative protein expression in Cav1-RFP versus control cell lines. Indicated proteins were assessed by Western blotting and normalized to β-actin. According to cavin nomenclature, PTRF is cavin-1, SRBC is cavin-2, and SDPR is cavin-3. *G*: Electron microscopy images of 3T3-L1 adipocytes transduced with an empty vector (*upper panel*) stably expressing Cav1-RFP (*middle panel*) or adipocytes of subcutaneous adipose tissue of mice (*lower panel*). Bar scale: 300 nm. *H*: Quantification of caveolae density from electron microscopy images. A total of 40-μm membrane stretches were used for caveolae quantification in each group using ImageJ software. Caveolae density is expressed as the number of invaginated caveolae per micrometer membrane length, and values are means ± SEM of 6–10 image sections. Significant differences between groups by Student *t* test are indicated as follows: ***$P < 0.001$, *$P < 0.05$.

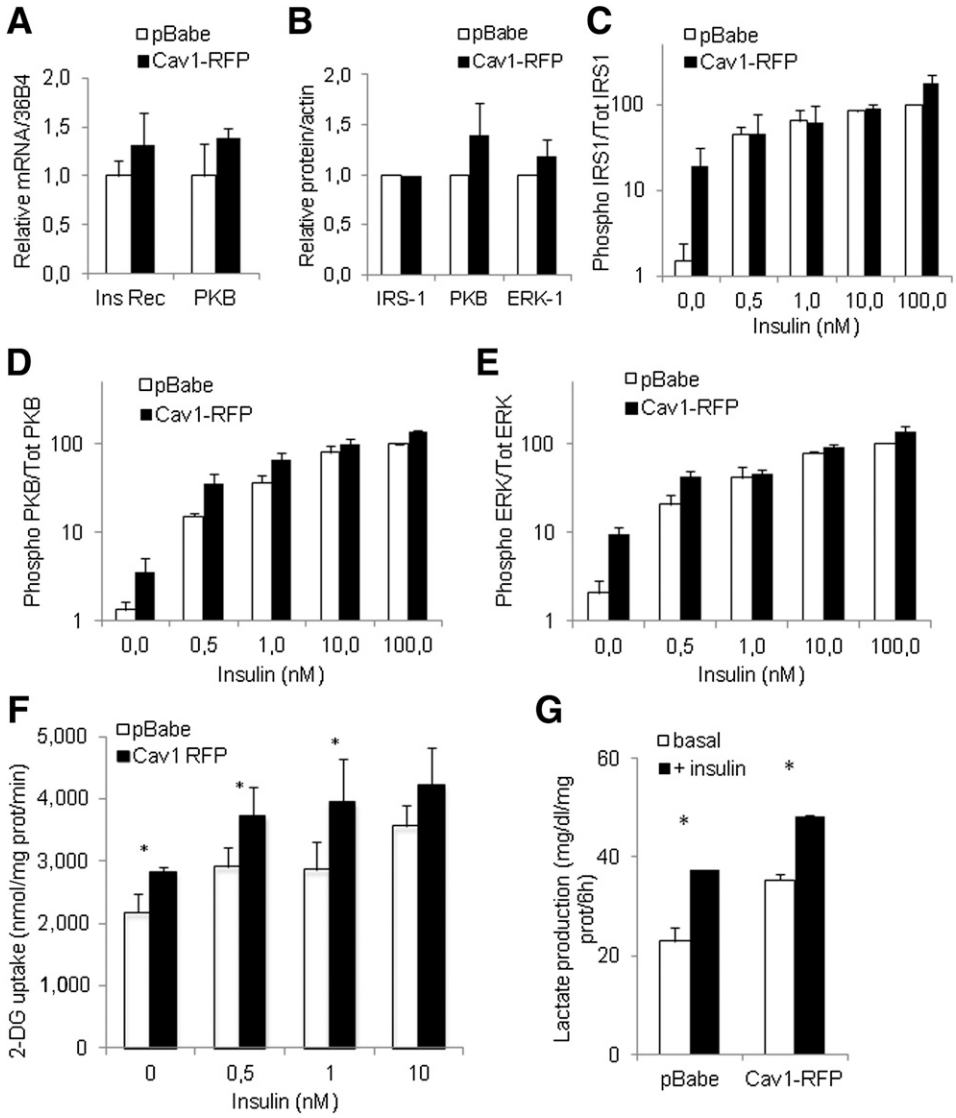

Figure 2—Caveolin-1 overexpression increases adipocyte basal metabolic activity. *A*: Expression of insulin receptor (Ins Rec) and PKB mRNA in control or Cav1-RFP differentiated adipocytes. 36B4 mRNA was used for normalization. *B*: Protein expression of IRS-1, PKB, and Erk1 in Cav1-RFP adipocytes. β-Actin normalization was used in Western blots. *C–E*: Insulin-dependent phosphorylation of PKB (phospho-Ser^{473}; Cell Signaling) or IRS-1 (phospho-Tyr^{612}; Upstate) and Erk1/2 (phospho-Thr^{202}/Tyr^{204}; Cell Signaling) was evaluated by Western blotting with phospho-specific antibodies, and signals were normalized to total protein (Tot). Incubation with indicated insulin concentrations was for 30 min, and total cell lysates were immediately frozen. Values are means ± SEM of four experiments in independent transfectants pools, expressed relative to values of maximally insulin-stimulated control cells. A log scale is used for dose-response curves. *F*: 2-Deoxyglucose (2-DG) transport was measured after overnight insulin deprivation. 2-DG (0.2 mmol/L) was added for 8 min, and reaction was stopped by addition of ice-cold buffer. Values are means ± SEM obtained in three independent experiments. *G*: Lactate production by control or Cav1-RFP adipocytes. Cells were exposed to insulin (100 nmol/L) for 6 h in fresh DMEM. Extracellular lactate concentration was measured using a commercial kit. *Significant differences by paired *t* test. prot, protein.

was increased both in basal and in insulin-stimulated states in Cav1-RFP (Fig. 2*G*), suggesting active metabolic activity by cav1 overexpression.

Caveolin Overexpression Increases Adipocyte Ability to Accommodate Larger Lipid Droplets in Cultured Cells and Mice

Metabolic changes in Cav1-RFP adipocytes suggest that they might deposit more lipids. Compared with control fat cells, size distribution of Oil Red O–stained lipid droplets from Cav1-RFP adipocytes was right shifted, indicating bigger lipid droplets in Cav1-RFP-caveolae–enriched cell lines (Fig. 3*A* and *B*). We also transduced parental 3T3-L1 adipocytes with an adenovirus encoding untagged caveolin-1, which almost doubled cav1 protein expression (Fig. 3*C*) and right shifted lipid droplet size distribution (Fig. 3*D*), further indicating that lipid droplet expansion by caveolin-1 overexpression was independent of the presence of the RFP tag. The extent of lipid droplet size enlargement in adenoviral experiments was

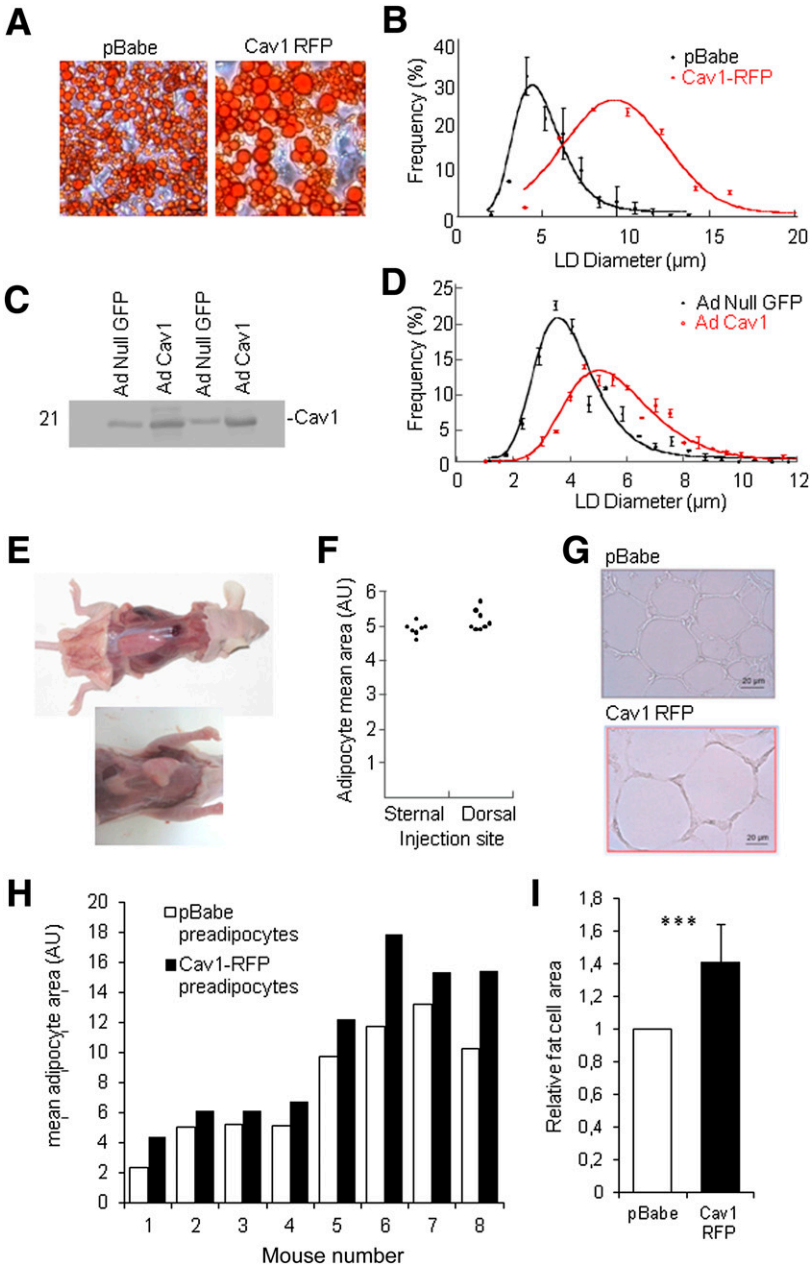

Figure 3—Caveolin-1 overexpression increases adipocyte lipid storage in cell culture and mice adipose tissue. *A*: Images of Oil Red O–stained cultured adipocytes transduced with an empty vector (pBabe) of stably expressing Cav1-RFP. *B*: Lipid droplet (LD) size distribution in control or Cav1-RFP stable 3T3-L1 clones. Lipid droplet size was measured on microscope images using ImageJ software. Mean distributions were calculated from values collected in four independent pools of stable 3T3-L1 clones and represent ~500 individual lipid droplets in each group. *C*: Untagged caveolin-1 overexpression in 3T3-L1 adipocytes by adenoviral vector encoding caveolin-1 (Ad Cav1) or GFP (Ad Null GFP). Two independent experiments are shown. *D*: Lipid droplet size distribution in adipocytes infected with Ad Cav1 or Ad Null GFP. *E*: 3T3-F442A preadipocytes (30×10^6 cells) were injected subcutaneously in the dorsal (*upper panel*) or the ventral (*lower panel*) region of 6-week-old nude mice. After 2 months with ad libitum feeding, mice were given access to 30% sucrose in drinking water for 2 weeks and killed. Newly formed fat pads are shown. *F* and *G*: Histological sections were prepared from newly formed fat pads, and mean adipocyte area was determined with ImageJ software. Values are mean of fat cell surface of individual mice receiving matched injections of control preadipocytes in the dorsal and ventral regions. *H*: Mean adipocyte area in newly formed fat pads from mice injected twice with control (pBabe) and Cav1-RFP–expressing preadipocytes. Data collected on eight individual mice are shown. *I*: Mean values for relative adipocyte area in control (pBabe) versus Cav1-RFP–derived fat pads. Paired Student *t* test indicated significant changes (***$P < 0.001$). AU, arbitrary units.

lower than that seen with stable retrovirus-based overexpression, likely because of limited duration of transgene expression (2 days versus 10 days).

To determine whether lipid droplet–promoting effects of caveolae enrichment was limited to cultured cells or could also be observed in vivo, we compared adipocytes generated in nude mice from control or Cav1-RFP stable transfectants injected subcutaneously according to an established protocol (33). In preliminary experiments, single mice received two separate injections with parental cell line in the dorsal and ventral regions, which generated fat pads with similar morphology and fat cell size in the two locations (Fig. 3*E*), indicating independent size of newly formed fat cells on the injection site (Fig. 3*F*). Then, stable transfectants (control empty vector and Cav1-RFP preadipocytes) were injected in eight mice, individually receiving the two different cell lines in the dorsal or ventral region to generate Cav1-RFP or control adipocytes in the same animal. Cav1-RFP expression could be recovered in newly formed fad pads confirming their exogenous origin (Supplementary Fig. 2*B*). Interindividual variability was found in ultimate fat cell size of newly formed fat pads (Fig. 3*G*), but within a single mouse we consistently found bigger fat cells in pads originating from Cav1-RFP preadipocytes (Fig. 3*G* and *H*), with a significant 1.5-fold increase in mean fat cell area in Cav1-RFP (Fig. 3*I*). All together, these data indicate that caveolae density of adipocyte membrane can modulate the ability of fat cells to accommodate lipids in vitro and in vivo.

Caveolin-1 Expression Correlates With Fat Cell Hypertrophic Response to Overfeeding in Healthy Humans

These data strongly suggest that caveolin-1 expression participates in the setting of adipocyte expandability, a key parameter in physiological response to nutrient overload. To address this, we assessed caveolin expression in adipose tissue frozen biopsies obtained from healthy human subjects enrolled in a trial designed to investigate metabolic effects of overfeeding. Thirty-five young subjects (6 females and 29 males) participated in the 8-week overfeeding protocol, and caveolin-1 protein expression showed no significant correlation with fat cell size at baseline (data not shown). During overfeeding, all the subjects gained weight (from 4.4 to 10.7 kg, mean value 7.5 kg) and increased fat mass as well as nonfat mass (Fig. 4*A*). Fat-cell size measurements at baseline and after overfeeding in each subject revealed two different patterns in the overfeeding response: 15 subjects increased the size of their fat cells (Fig. 4*B*), whereas it remained unchanged or even decreased in 20 subjects (Fig. 4*C*). Since total fat mass similarly increased in the two groups during the overfeeding period, this was indicative of different patterns of adipose tissue response dominated either by hyperplastic (increase in adipocyte number) or hypertrophic (increase in adipocyte lipid droplet size) expansion. In subjects responding to overfeeding by adipocyte enlargement, we found that caveolin-1 protein expression at baseline positively correlated with the change in fat cell size (Fig. 4*D*), whereas no association was observed in hyperplastic responders. Thus, in healthy humans, adipocyte caveolin-1 is positively associated with the ability to expand fat cells in the face of nutrient overload.

Lipid Droplet Shrinkage Induces Caveolae Disassembly by Targeting Cavin Protein Stability

We established high expansion capacity in adipocytes with dense caveolae membranes and next investigated reciprocal relation associated with lipid droplet reduction. We used an experimental setting in which acute lipid droplet shrinkage was induced by prolonged stimulation of lipolysis by cAMP/protein kinase A activation. 3T3-L1 fully differentiated adipocytes were treated with lipolytic agents, 8Br-cAMP (a stable cAMP analog) or forskolin (FSK) (an adenylate cyclase activator), combined with methylisobutylxantine (MIX) (a cAMP-degrading phosphodiesterase inhibitor). Prolonged treatment (30 h) did not affected cell density or viability (Supplementary Fig. 3) but resulted in robust lipolytic stimulation (six- to eightfold) as judged by the release of triacylglycerol-derived glycerol (Fig. 5*A*). In this setting, almost constant lipolytic rates were observed (Fig. 5*A*), which led to markedly smaller lipid droplets by staining with LD540, a fluorescent neutral lipid probe (Fig. 5*B*). Striking reshaping of the plasma membrane was evident in adipocytes treated for 30 h with 8Br-cAMP, which almost completely lacked invaginated caveolae, whereas they were normally found in control cells (Fig. 5*C*). Quantitative analysis of electron microscopy images confirmed drastic reduction of caveolae density by 8Br-cAMP treatment (Fig. 5*D*). Reduction of caveolae number was also observed in adipose tissue electron microscopy sections of mice induced for adipose tissue mobilization by 48-h fasting (Fig. 5*E*).

To investigate the mechanism of caveolae disassembly, we focused on the main caveolar coat component, caveolin-1, and observed no sign of decline upon prolonged lipolytic stimulation (Fig. 6*A*). Instead, total caveolin protein accumulated in 8Br-cAMP–treated cells from 18 h onwards, resulting in a two- to threefold higher content at end point (Fig. 6*B*). A similar response was observed using FSK and MIX suggesting a cAMP-mediated event (Fig. 6*C*). This is in agreement with increased caveolin contents already reported in adipose tissue of rodents during fasting (34). Therefore, loss of caveolin protein is unlikely to explain disappearance of caveolae after prolonged lipid mobilization. As caveolae structures are dependent on cholesterol and caveolins are cholesterol-binding proteins (3), we next compared free cholesterol content in 8Br-cAMP– or FSK/MIX-treated adipocytes and found no change, suggesting a process independent of membrane cholesterol reduction (Fig. 6*D*). However, immunofluorescence revealed marked changes in caveolin-1 distribution, which evolved from a thin continuous labeling at cell periphery in control cells to a broken irregular pattern in 8Br-cAMP–treated

A

	Hyperplastic response group		Hypertrophic response group		
	Mean	sem	Mean	sem	pvalue
Number of subjects	20		15		
Age (years)	26,7	±6,1	26,7	±4,5	0,964184
Baseline					
Weight (kg)	81,9	±9,1	77,8	±10,3	0,250822
BMI (Kg/m2)	26,5	±2,5	24,8	±1,6	0,019444
Fat mass	19,3	±5,1	15,6	±4,6	0,038206
Fat-free mass	62,6	±10,7	62,2	±10,2	0,915438
Adipocyte volume (pl)	0,9	±0,4	0,6	±0,3	0,067008
Post overfeeding					
Weight (kg)	89,1	±10,1	85,5	±10,4	0,321831
BMI (Kg/m2)	29,0	±3,1	27,2	±1,6	0,034342
Fat mass	23,2	±6,2	20,0	±5,0	0,103070
Fat-free mass	65,9	±10,8	65,5	±10,4	0,924579
Adipocyte volume (pl)	0,8	±0,3	1,2	±0,3	0,000214
Overfeeding vs Baseline					
Delta BMI	2,5	±1,0	2,4	±0,8	0,761907
Delta fat mass	4,0	±1,5	4,3	±1,1	0,444650
Delta fat free mass	3,3	±1,1	3,4	±1,5	0,939271
Delta fat cell size	-0,1	±0,2	0,6	±0,2	0,000000

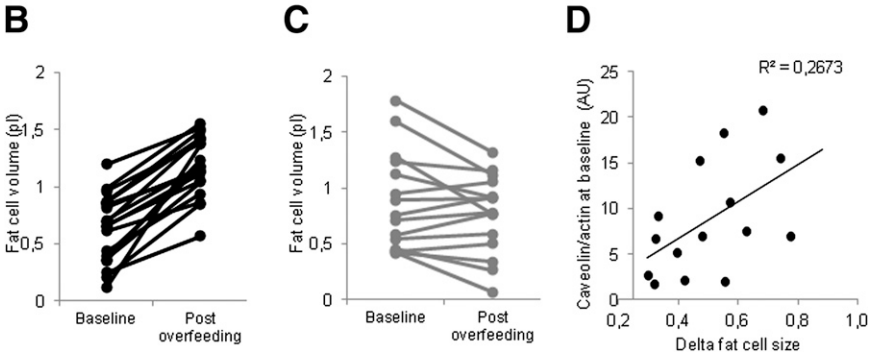

Figure 4—Caveolin expression and adipose tissue expansion during overfeeding in healthy subjects. *A*: Clinical parameters of subjects participating in the 8-week overfeeding protocol are described in RESEARCH DESIGN AND METHODS. The rational for group assignment is from the analysis of fat cell size change from preoverfeeding (baseline) to postoverfeeding, which defines hypertrophic (*B*) or hyperplastic (*C*) responses in individual patients. *D*: Spearman correlation of caveolin adipose tissue content to change in fat cell size in patients with hypertrophic response to overfeeding. Caveolin-1 content was assessed by Western blotting from total protein lysates (15 μg). β-Actin was used for normalization. AU, arbitrary units.

adipocytes, consistent with disappearance of surface caveolae structures (Fig. 6*E*). Therefore, we next examined the possibility that cavin adaptors, which are required for caveolae assembly, might be targeted during lipid droplet shrinkage. In time course experiments, PTRF/cavin-1 and SDPR/cavin-2 markedly changed upon 8Br-cAMP treatment (Fig. 7*A*). PTRF/cavin-1 showed a biphasic response to 8Br-cAMP with a transient increase within the first 12 h, followed by a rapid decline at later time points (Fig. 7*B*). SDPR/cavin-2 also markedly declined after 12 h with 8Br-cAMP but did not increase at shorter times (Fig. 7*C*). We also noticed a similar response of another noncavin protein, EHD2, which also drastically decreased with 8Br-cAMP (Fig. 7*D*). EHD2 is a dynamin-related ATPase (35) involved in many aspects of membrane dynamics (36). It colocalizes with caveolin-1 (37), interacts with cavin-1 (38), associates with caveolae (14), and links caveolae to actin filaments (39). FSK/MIX fully mimicked the 8Br-cAMP effect in reducing PTRF/cavin-1, SDPR/cavin-2, and EHD2 contents at end points (Fig. 7*E*). To test for decreased cavin protein stability, we used cavin-GFP reporters stably expressed in 3T3-L1. In this setting, fluorescent cavins are transcribed from a constitutive strong promoter, and changes in cell fluorescence intensity reflect protein stability. In 8Br-cAMP–treated adipocytes, lipid droplet shrinkage (see the information on LD540 staining) coincided with a drop in fluorescence intensity of PTRF-GFP (Fig. 7*F*) and SRBC-GFP (Fig. 7*G*), whereas caveolin-1–RFP remained unaltered (Fig. 6*H* and *I*). We also observed that PTRF/cavin-1 loss could be prevented by addition of a proteasome inhibitor MG132 (Supplementary Fig. 4*A*). These data demonstrate posttranslational regulation of PTRF/cavin-1 and SRBC/cavin-2 by 8Br-cAMP and identify cavin protein degradation, likely through proteasome, as a key process for cavin loss and caveolae disassembly upon adipocyte lipid mobilization. We also noticed significant reduction in SDPR/cavin-3 and EHD2 mRNA in 8Br-cAMP–treated cells (Supplementary Fig. 4*B*), indicating that transcriptional regulation might additionally contribute to the loss of some caveolar proteins.

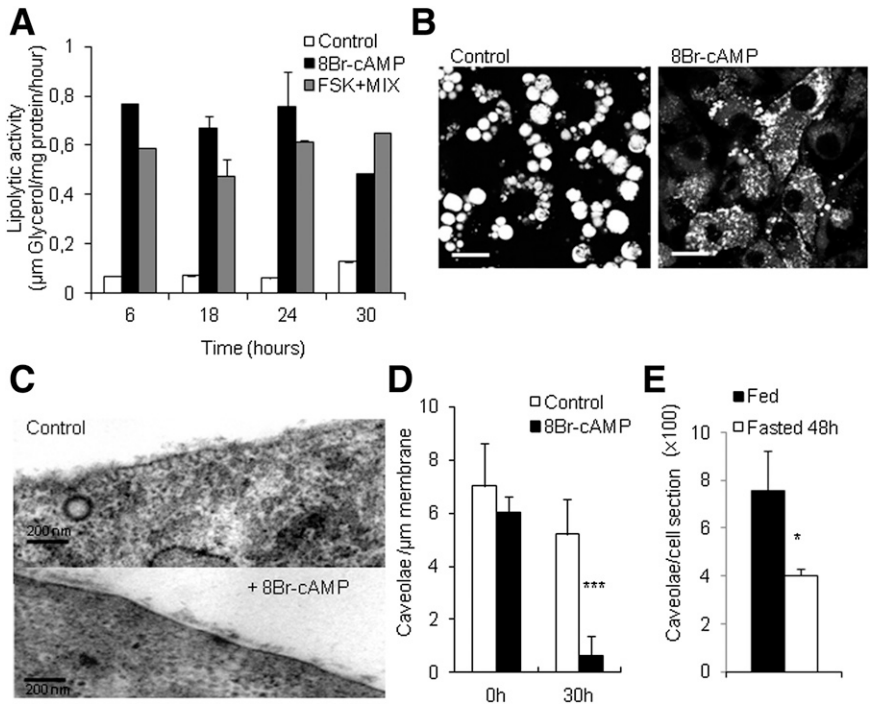

Figure 5—Lipid droplet shrinkage in 3T3-L1 adipocytes coincides with caveolae disassembly. *A*: Terminally differentiated 3T3-L1 adipocytes were cultured in DMEM supplemented with 10% FBS and treated with 1 mmol/L 8Br-cAMP or a combination of 10 μmol/L FSK and 500 μmol/L MIX. Rates of glycerol release to the extracellular medium (expressed per hour and per milligram cell protein) were measured for 2 h at indicated times over a 30-h period. Values are means ± SEM from four independent experiments. *B*: LD540 staining of neutral lipids in 3T3-L1 control adipocytes or cells treated for 30 h with 8Br-cAMP. Smaller lipid droplets after 8Br-cAMP denote effective lipid mobilization. Bar scale: 20 μm. *C*: Electron microscopy images of control or 8Br-cAMP–treated 3T3-L1 adipocytes. Note the presence of abundant caveolae on the surface of control cells only. Bar scale: 200 nm. *D*: Quantification of caveolae density from electron microscopy images. Caveolae invaginations were counted on linear membrane stretches representing a total of 30 μm membrane length in 6–10 images from different sections using ImageJ. Data represent means ± SEM (***$P < 0.001$). *E*: Caveolae quantification on electron microscopy adipose tissue sections of mice fasted for 48 h or fed (three mice per group). Caveolae number was compared on a per-cell basis (expressed as 100 caveolae/length of membrane perimeter). Data are means ± SEM. *$P < 0.05$.

DISCUSSION

Our data establish reciprocal relationship linking caveolae dynamics and lipid store fluctuations in adipocytes and define the key steps in cavin/caveolin balance for adaptive maintenance of fat cell caveolae. We demonstrate that caveolar density can be raised by enforced adipocyte caveolin-1 expression, which promotes fat cell expandability through ameliorated insulin response. Furthermore, we found that adipose tissue caveolin-1 expression specifically associated with hypertrophic (and not hyperplastic) fat tissue expansion in healthy human subjects challenged by overfeeding. Conversely, lipid droplet shrinkage by sustained mobilization is shown here to ultimately produce the disassembly of caveolae through cavin-dependent protein degradation. Therefore, our findings highlight bidirectional lipid droplet to membrane cross-talk for the maintenance of fat cell metabolic flexibility and adaptation to highly variable metabolic conditions primarily impacting lipid droplet volume to ultimately resolve fat cell size. They indicate membrane dynamic response to fat storage, in which continuous caveolae formation (through caveolin-1–regulated expression) is required for fat cell membrane expansion, whereas lipid droplet shrinking associates with intensive remodeling (driven by cavin protein targeting) and caveolae disassembly needed to adapt membrane excess. Our observations fit with a prevailing role of caveolae as sensors of cell membrane tension and also suggest a new aspect of lipid droplets as mechano-active organelles driving membrane stretching, at least when of sufficient size as found in adipocytes. In line, a vimentin network tightly enwrapping adipocyte lipid droplets was identified in early morphological studies (40), and recent proteomic analysis of lipid droplets revealed association with cytoskeleton and molecular motors components (29,41–43). All together, these observations contribute to expand the fast-growing list of lipid droplet–related processes related to cell architecture (rev. in 44).

Our study underlines the importance of caveolae density to promote fat cell expandability, a question with physio-pathological relevance in the context of epidemic development of metabolic diseases worldwide. As a hallmark of obesity, lipid droplet expansion defines adipocyte hypertrophy, and a prevailing view is that saturation of adipose tissue storage leads to the spillover and dissemination of fatty acids to contribute to multiorgan metabolic complications. Therefore, identification of cellular effectors

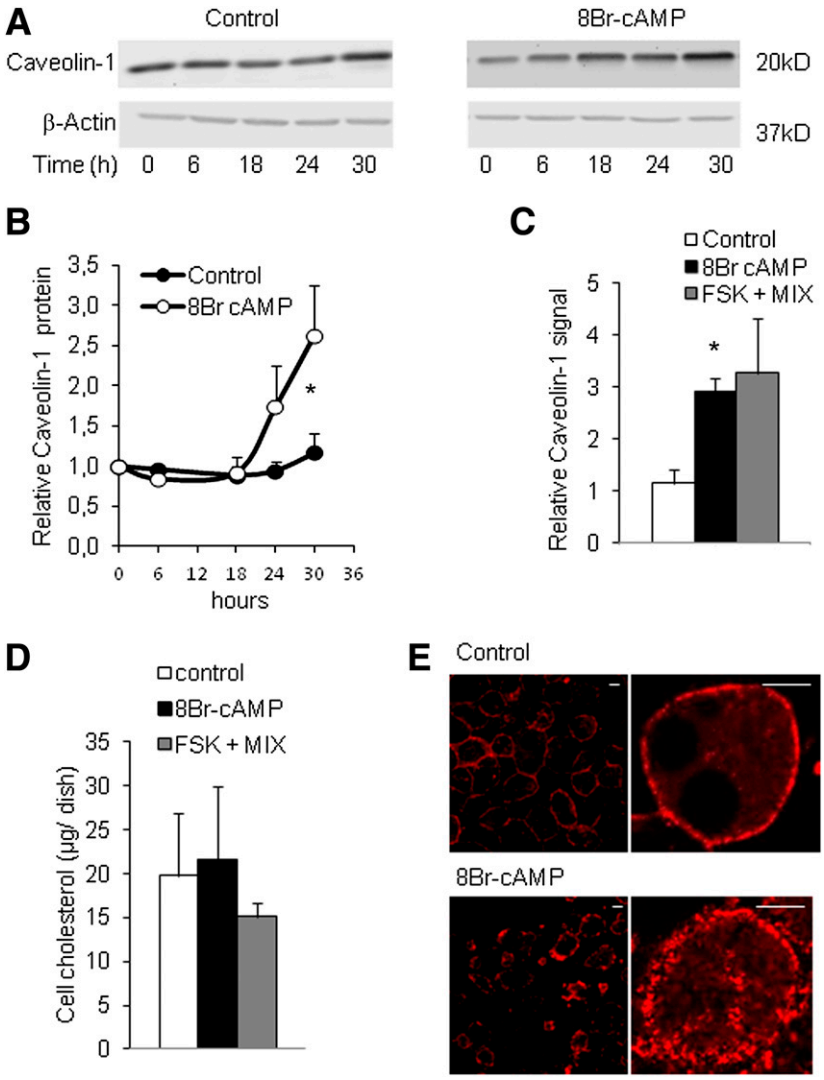

Figure 6—Effect of prolonged lipid mobilization by 8Br-cAMP on caveolin-1. *A*: Time course of 8Br-cAMP exposure on caveolin-1 protein contents in 3T3-L1 adipocytes. β-Actin is used as a loading control for Western blot analysis. *B* and *C*: Quantitative analysis of caveolin-1 protein expression in control adipocytes or cells treated with 1 mmol/L 8Br-cAMP for 30 h (*B*) or at end point (*C*). Values are obtained by densitometric scanning of immunoblots and expressed relative to initial protein signals. Means ± SEM from 3–5 independent experiments are shown. *Significant difference by Student *t* test ($P < 0.05$). *D*: Adipocyte lysates were used to determine free cholesterol content. Mean values ± SEM were obtained from three independent experiments. *E*: Immunofluorescence labeling of endogenous caveolin-1 in differentiated 3T3-L1 adipocytes untreated (*upper panel*) or treated with 8Br-cAMP for 30 h (*lower panel*). Bar scale is 5 μm.

participating in the control of adipocyte lipid storage is of interest to target fatty acid lipotoxic effects. Although it was recognized for long that lack of caveolae severely compromises fat cell expansion as seen in lipoatrophic diabetic caveolin-deficient patients (9,17), caveolar protein expression is not generally associated with obesity, suggesting that steady-state caveolae is globally maintained in obese animals or humans. In agreement, a recent study of caveolin-1 and cavin-1 expression in single adipocytes established a close correlation with their cell surface area (45). Here, we bring evidence that adipocyte caveolae, rather, serve in the adaptation to lipid store fluctuations contributing to fat cell flexibility and provide a scheme for adipocyte caveolin/cavin protein interplay in this adaptive response. During fat storage, membrane surface growth is required for adipocyte expansion, and caveolin-1 expression is rate limiting for additional caveolae formation whereas cavin-1 can be recruited from noncaveolar pools. Noteworthy, adipocyte PTRF/cavin-1 is not restricted to caveolae but also associates with nonraft membranes (Supplementary Fig. 1*C*) as well as lipid droplets (29), which likely provide reservoirs. During extreme fat cell shrinkage, cavins are targeted to degradation, an event reported in other cell types and conditions as instrumental to signal caveolae disassembly (23). Lipid mobilization is shown here to induce a complex biphasic response of cavin-1. Acutely, PTRF/cavin-1

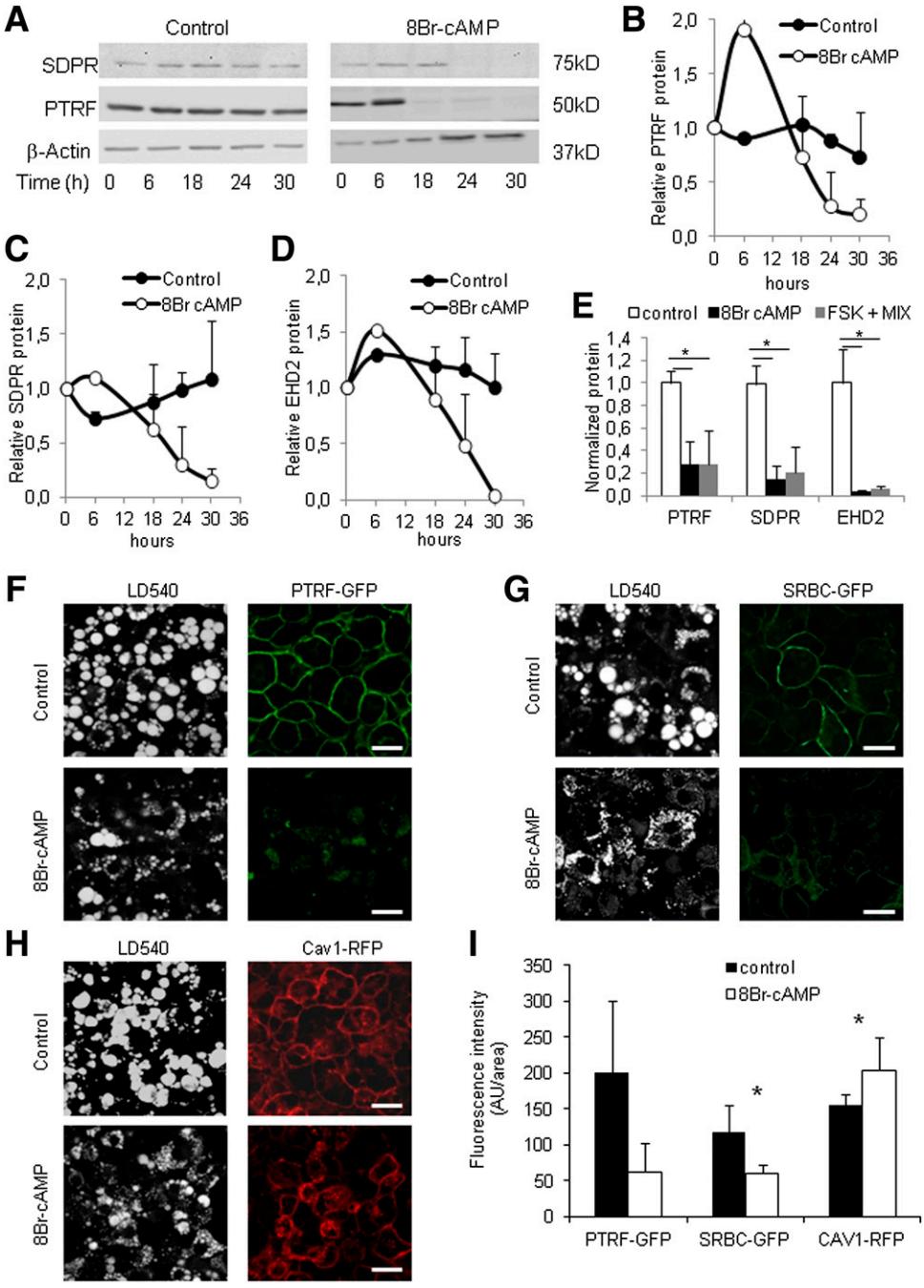

Figure 7—Prolonged lipid mobilization by 8Br-cAMP induces loss of cavins by protein degradation. *A*: Time course of 8Br-cAMP exposure on PTRF/cavin-1 and SDPR/cavin-2 protein contents in 3T3-L1 adipocytes. Fully differentiated adipocytes were treated or not with 1 mmol/L 8Br-cAMP as described above. β-Actin is used as a loading control. *B–E*: Quantitative changes in PTRF/cavin-1 (*B*), SDPR/cavin-2 (*C*), and EHD2 (*D*) protein expression with 8Br-cAMP treatment or at end point (30 h) with no effector (control), 1 mmol/L 8Br-cAMP, a combination of 10 μmol/L FSK and 500 μmol/L MIX, or 10 μmol/L FSK alone (*E*). Values are obtained by densitometric scanning of immunoblots and expressed relative to initial protein signals. Means ± SEM from at least three to five independent experiments are shown. *Significant difference by *t* test ($P < 0.05$). *F–I*: Fully differentiated 3T3-L1 adipocytes stably expressing PTRF-GFP (*F*), SRBC-GFP (*G*), or Cav1-RFP (*H*) were treated or not with 1 mmol/L 8Br-cAMP for 30 h. Lipids were stained using the neutral lipid probe LD540, and cells were analyzed by confocal microscopy (bar scale: 20 μm). Fluorescence intensity of confocal images (*I*) was evaluated using ImageJ software. Ten to 12 confocal images from different microscopic fields were acquired in the different cell lines. The sum of the fluorescence intensity was divided by microscopic field area. Data represent means ± SEM (*$P < 0.05$). AU, arbitrary units.

protein content increases, as well as caveolin-1, in agreement with that reported in fasting mice adipose tissue (34,46). Only in later phases, when lipid store shrinks, do cavin proteins and caveolin-1 become differentially regulated and caveolae ultimately disassemble. Whether PTRF/cavin-1 biphasic response is linked to phosphorylation on serine residues, recently demonstrated upon acute cAMP/PKA activation (46), or can be induced after PKG stimulation, another lipolytic pathway in adipocytes (47) remains to be established. Furthermore, we cannot exclude that the loss of EHD2, which is observed within a similar time frame, may also be an upstream molecular event in caveolae disassembly by lipid droplet shrinkage. Indeed, depletion of EHD2 was recently shown to result in more dynamic and short-lived caveolae (38).

Lastly, this study provides evidence that raising caveolae density can ameliorate adipocyte metabolic response and provides indications that this is achieved through raising basal as well as insulin-stimulated effects. This is in line with previous observations with caveolin-1 modulation by miRNAs (48), mirroring a state of metabolic inflexibility in caveolae-deficient mice models by either caveolin-1 or cavin-1 knockout (49,50). In line, one study also reported that mice hepatocytes, which normally express very low caveolin, could be sensitized for insulin action by exogenous caveolin-3 expression (51).

To conclude, our present data establish fat cell caveolae function in a unique cell response to lipid store variation suggesting lipid-induced mechanotension. Even if caveolae response to mechanotension has been described to occur within minutes, kinetics of lipid-induced mechanotension in adipocytes may be somewhat slower but might involve similar end point responses. On the whole, intervention on caveolin/cavin protein balance might be metabolically beneficial to optimize fat storage into adipocytes.

Acknowledgments. Kai Simons (MPI-CBG, Dresden, Germany) provided adenovirus encoding canine Cav1. Plasmids encoding Cav1-RFP, PTRF-eGFP, and SRBC-eGFP were generously provided, respectively, by R.G. Parton (Institute for Molecular Biosciences, University of Queensland, Brisbane, Australia) and R.G. Anderson (Department of Cell Biology, University of Texas Southwestern Medical Center, Dallas, TX).

Funding. Funding from European Community FP7/2007-2013 LipidomicNet grant agreement no. 202272 and from NORC grant no. P30DK072476 (National Institutes of Health–National Institute of Diabetes and Digestive and Kidney Diseases) is acknowledged. S.L.L. is funded by a grant from "Region Pays de la Loire."

Duality of Interest. No potential conflicts of interest relevant to this article were reported.

Author Contributions. N.B. researched data and reviewed and edited the manuscript. C.P., G.M., F.L., X.L.L., and J.D.C. researched data. E.R. contributed to discussion and reviewed and edited the manuscript. S.L.L. and I.D. wrote the manuscript and researched data. S.L.L. and I.D. are the guarantors of this work and, as such, had full access to all the data in the study and take responsibility for the integrity of the data and the accuracy of the data analysis.

References

1. Palade GE. Blood capillaries of the heart and other organs. Circulation 1961; 24:368–388
2. Parton RG, Simons K. The multiple faces of caveolae. Nat Rev Mol Cell Biol 2007;8:185–194
3. Rothberg KG, Heuser JE, Donzell WC, Ying YS, Glenney JR, Anderson RG. Caveolin, a protein component of caveolae membrane coats. Cell 1992;68:673–682
4. Le Lay S, Kurzchalia TV. Getting rid of caveolins: phenotypes of caveolin-deficient animals. Biochim Biophys Acta 2005;1746:322–333
5. Razani B, Engelman JA, Wang XB, et al. Caveolin-1 null mice are viable but show evidence of hyperproliferative and vascular abnormalities. J Biol Chem 2001;276:38121–38138
6. Drab M, Verkade P, Elger M, et al. Loss of caveolae, vascular dysfunction, and pulmonary defects in caveolin-1 gene-disrupted mice. Science 2001;293: 2449–2452
7. Razani B, Combs TP, Wang XB, et al. Caveolin-1-deficient mice are lean, resistant to diet-induced obesity, and show hypertriglyceridemia with adipocyte abnormalities. J Biol Chem 2002;277:8635–8647
8. Briand N, Le Lay S, Sessa WC, Ferré P, Dugail I. Distinct roles of endothelial and adipocyte caveolin-1 in macrophage infiltration and adipose tissue metabolic activity. Diabetes 2011;60:448–453
9. Kim CA, Delépine M, Boutet E, et al. Association of a homozygous nonsense caveolin-1 mutation with Berardinelli-Seip congenital lipodystrophy. J Clin Endocrinol Metab 2008;93:1129–1134
10. Yu J, Bergaya S, Murata T, et al. Direct evidence for the role of caveolin-1 and caveolae in mechanotransduction and remodeling of blood vessels. J Clin Invest 2006;116:1284–1291
11. Sinha B, Köster D, Ruez R, et al. Cells respond to mechanical stress by rapid disassembly of caveolae. Cell 2011;144:402–413
12. Hill MM, Bastiani M, Luetterforst R, et al. PTRF-Cavin, a conserved cytoplasmic protein required for caveola formation and function. Cell 2008;132:113–124
13. Liu L, Pilch PF. A critical role of cavin (polymerase I and transcript release factor) in caveolae formation and organization. J Biol Chem 2008;283:4314–4322
14. Aboulaich N, Vainonen JP, Strålfors P, Vener AV. Vectorial proteomics reveal targeting, phosphorylation and specific fragmentation of polymerase I and transcript release factor (PTRF) at the surface of caveolae in human adipocytes. Biochem J 2004;383:237–248
15. Liu L, Brown D, McKee M, et al. Deletion of Cavin/PTRF causes global loss of caveolae, dyslipidemia, and glucose intolerance. Cell Metab 2008;8:310–317
16. Hayashi YK, Matsuda C, Ogawa M, et al. Human PTRF mutations cause secondary deficiency of caveolins resulting in muscular dystrophy with generalized lipodystrophy. J Clin Invest 2009;119:2623–2633
17. Shastry S, Delgado MR, Dirik E, Turkmen M, Agarwal AK, Garg A. Congenital generalized lipodystrophy, type 4 (CGL4) associated with myopathy due to novel PTRF mutations. Am J Med Genet A 2010;152A:2245–2253
18. Rajab A, Straub V, McCann LJ, et al. Fatal cardiac arrhythmia and long-QT syndrome in a new form of congenital generalized lipodystrophy with muscle rippling (CGL4) due to PTRF-CAVIN mutations. PLoS Genet 2010;6:e1000874
19. Gazzerro E, Sotgia F, Bruno C, Lisanti MP, Minetti C. Caveolinopathies: from the biology of caveolin-3 to human diseases. Eur J Hum Genet 2010;18:137–145
20. Verma P, Ostermeyer-Fay AG, Brown DA. Caveolin-1 induces formation of membrane tubules that sense actomyosin tension and are inhibited by polymerase I and transcript release factor/cavin-1. Mol Biol Cell 2010;21:2226–2240
21. Hansen CG, Bright NA, Howard G, Nichols BJ. SDPR induces membrane curvature and functions in the formation of caveolae. Nat Cell Biol 2009;11:807–814
22. McMahon KA, Zajicek H, Li WP, et al. SRBC/cavin-3 is a caveolin adapter protein that regulates caveolae function. EMBO J 2009;28:1001–1015
23. Hansen CG, Shvets E, Howard G, Riento K, Nichols BJ. Deletion of cavin genes reveals tissue-specific mechanisms for morphogenesis of endothelial caveolae. Nat Commun 2013;4:1831

24. Briand N, Dugail I, Le Lay S. Cavin proteins: New players in the caveolae field. Biochimie 2011;93:71–77
25. Thorn H, Stenkula KG, Karlsson M, et al. Cell surface orifices of caveolae and localization of caveolin to the necks of caveolae in adipocytes. Mol Biol Cell 2003;14:3967–3976
26. Hirsch J, Gallian E. Methods for the determination of adipose cell size in man and animals. J Lipid Res 1968;9:110–119
27. Hainque B, Guerre-Millo M, Hainault I, Moustaid N, Wardzala LJ, Lavau M. Long term regulation of glucose transporters by insulin in mature 3T3-F442A adipose cells. Differential effects on two glucose transporter subtypes. J Biol Chem 1990;265:7982–7986
28. Le Lay S, Robichon C, Le Liepvre X, Dagher G, Ferre P, Dugail I. Regulation of ABCA1 expression and cholesterol efflux during adipose differentiation of 3T3-L1 cells. J Lipid Res 2003;44:1499–1507
29. Blouin CM, Le Lay S, Eberl A, et al. Lipid droplet analysis in caveolin-deficient adipocytes: alterations in surface phospholipid composition and maturation defects. J Lipid Res 2010;51:945–956
30. Tondu AL, Robichon C, Yvan-Charvet L, et al. Insulin and angiotensin II induce the translocation of scavenger receptor class B, type I from intracellular sites to the plasma membrane of adipocytes. J Biol Chem 2005;280:33536–33540
31. Le Lay S, Briand N, Blouin CM, et al. The lipoatrophic caveolin-1 deficient mouse model reveals autophagy in mature adipocytes. Autophagy 2010;6:754–763
32. Nichols BJ, Kenworthy AK, Polishchuk RS, et al. Rapid cycling of lipid raft markers between the cell surface and Golgi complex. J Cell Biol 2001;153:529–541
33. Mandrup S, Loftus TM, MacDougald OA, Kuhajda FP, Lane MD. Obese gene expression at in vivo levels by fat pads derived from s.c. implanted 3T3-F442A preadipocytes. Proc Natl Acad Sci U S A 1997;94:4300–4305
34. Cohen AW, Razani B, Schubert W, et al. Role of caveolin-1 in the modulation of lipolysis and lipid droplet formation. Diabetes 2004;53:1261–1270
35. Daumke O, Lundmark R, Vallis Y, Martens S, Butler PJ, McMahon HT. Architectural and mechanistic insights into an EHD ATPase involved in membrane remodelling. Nature 2007;449:923–927
36. Guilherme A, Soriano NA, Bose S, et al. EHD2 and the novel EH domain binding protein EHBP1 couple endocytosis to the actin cytoskeleton. J Biol Chem 2004;279:10593–10605
37. Hansen CG, Howard G, Nichols BJ. Pacsin 2 is recruited to caveolae and functions in caveolar biogenesis. J Cell Sci 2011;124:2777–2785
38. Morén B, Shah C, Howes MT, et al. EHD2 regulates caveolar dynamics via ATP-driven targeting and oligomerization. Mol Biol Cell 2012;23:1316–1329
39. Stoeber M, Stoeck IK, Hänni C, Bleck CKE, Balistreri G, Helenius A. Oligomers of the ATPase EHD2 confine caveolae to the plasma membrane through association with actin. EMBO J 2012;31:2350–2364
40. Franke WW, Hergt M, Grund C. Rearrangement of the vimentin cytoskeleton during adipose conversion: formation of an intermediate filament cage around lipid globules. Cell 1987;49:131–141
41. Brasaemle DL, Dolios G, Shapiro L, Wang R. Proteomic analysis of proteins associated with lipid droplets of basal and lipolytically stimulated 3T3-L1 adipocytes. J Biol Chem 2004;279:46835–46842
42. Bartz R, Zehmer JK, Zhu M, et al. Dynamic activity of lipid droplets: protein phosphorylation and GTP-mediated protein translocation. J Proteome Res 2007;6:3256–3265
43. Yu YV, Li Z, Rizzo NP, Einstein J, Welte MA. Targeting the motor regulator Klar to lipid droplets. BMC Cell Biol 2011;12:9
44. Farese RV Jr, Walther TC. Lipid droplets finally get a little R-E-S-P-E-C-T. Cell 2009;139:855–860
45. Hulstrøm V, Prats C, Vinten J. Adipocyte size and cellular expression of caveolar proteins analyzed by confocal microscopy. Am J Physiol Cell Physiol 2013;304:C1168–C1175
46. Aboulaich N, Chui PC, Asara JM, Flier JS, Maratos-Flier E. Polymerase I and transcript release factor regulates lipolysis via a phosphorylation-dependent mechanism. Diabetes 2011;60:757–765
47. Lafontan M, Moro C, Berlan M, Crampes F, Sengenes C, Galitzky J. Control of lipolysis by natriuretic peptides and cyclic GMP. Trends Endocrinol Metab 2008;19:130–137
48. Trajkovski M, Hausser J, Soutschek J, et al. MicroRNAs 103 and 107 regulate insulin sensitivity. Nature 2011;474:649–653
49. Asterholm IW, Mundy DI, Weng J, Anderson RG, Scherer PE. Altered mitochondrial function and metabolic inflexibility associated with loss of caveolin-1. Cell Metab 2012;15:171–185
50. Ding SY, Lee MJ, Summer R, Liu L, Fried SK, Pilch PF. Pleiotropic effects of cavin-1 deficiency on lipid metabolism. J Biol Chem 2014;289:8473–8483
51. Otsu K, Toya Y, Oshikawa J, et al. Caveolin gene transfer improves glucose metabolism in diabetic mice. Am J Physiol Cell Physiol 2010;298:C450–C456